

Luminescence properties and defects in GaN nanocolumns grown by molecular beam epitaxy

E. Calleja, M. A. Sánchez-García, F. J. Sánchez, F. Calle, F. B. Naranjo, and E. Muñoz
Departamento Ingeniería Electrónica, ETSI Telecomunicación, Universidad Politécnica, 28040 Madrid, Spain

U. Jahn and K. Ploog
Paul Drude Institut für Festkörperelektronik, Hausvogteiplatz 5-7, D-10117 Berlin, Germany
 (Received 17 May 2000)

Wurtzite GaN nanocolumns are reproducibly grown by plasma-assisted molecular beam epitaxy on Si(111) and *c*-sapphire substrates. The nanocolumns density and diameter (600–1500 Å) are effectively controlled by means of the III/V ratio. The nanocolumns are fully relaxed from lattice and thermal strain, having a very good crystal quality characterized by strong and narrow (2 meV) low-temperature photoluminescence excitonic lines at 3.472–3.478 eV. In addition, the spectra reveal a doublet at 3.452–3.458 eV and a broad line centered at 3.41 eV. This broad emission shows a sample-dependent spectral energy dispersion, from 3.40 to 3.42 eV, explained as due to the effect of strain and/or electric fields associated with extended structural defects located at the nanocolumns bottom interface. From cathodoluminescence data, it is concluded that the doublet emission lines originate at the nanocolumns volume, most probably related to Ga_i defects, given the column growth mode (Ga balling).

I. INTRODUCTION

Wurtzite GaN and its alloys with Al and In are largely exploited for commercial fabrication of blue light-emitting diodes and room-temperature cw operating lasers with lifetimes over 10 000 h.¹ Despite these technological advances, the generation and electronic structure of defects in GaN layers and their effects on device properties are still unclear. There is very little evidence of the presence of these defects in GaN from experimental data, as well as about their contribution to the photoluminescence (PL) emissions. Besides, it is difficult to identify which contributions belong to a given structural defect in a material where high densities of dislocations, point defects, and impurities are present, so that, the need of a very good crystal quality, as a starting point for these experiments, is evident. In addition, a method to grow high-quality, ordered nanostructures brings a unique tool to study new phenomena and opens up new insights for device applications.

This work studies the low-temperature PL emissions in relation with the morphology, growth conditions, and structural defects in high crystal quality GaN nanocolumns grown by molecular beam epitaxy (MBE) on Si(111) and sapphire substrates. Continuous-wave and time-resolved PL, Raman scattering (RS), cathodoluminescence (CL), and scanning electron microscopy (SEM) techniques are used to analyze the presence of defects in GaN nanocolumns.

II. EXPERIMENT

Wurtzite GaN epitaxial nanocolumns were grown by MBE on high-resistivity (50–400 Ω cm) Si(111), with and without high-temperature (800 °C) AlN buffer, as well as on *c*-sapphire substrates using low-temperature (500 °C) GaN buffers. All GaN crystals were grown at 770 °C under different III/V ratios. A cryogenically cooled rf plasma source (Oxford Applied Research CARS25) supplied the active ni-

trogen, allowing a maximum growth rate of 0.5 μm/h. A detailed description of the growth system and method can be found elsewhere.^{2,3}

Continuous-wave PL, excited with the 334-nm line of an Ar⁺ laser, was dispersed by a Jobin-Yvon THR 1000 monochromator and detected with a UV-enhanced GaAs photomultiplier and a lock-in amplifier. Time-resolved PL was measured with a frequency-doubled Ti-sapphire laser under 200-fs pulses (peak power of 0.2 MW/cm²) pumped with a mode-locked Ar⁺ laser having a time resolution of 100 ps. Cathodoluminescence was performed in a SEM equipped with an Oxford Mono-CL and a He-cooling stage (5–300 K range). The electron beam had energies from 5 to 25 keV with a current of 0.1 nA. RS measurements were carried out using a Spex 1404 double grating spectrometer with a multichannel detector.

III. RESULTS AND DISCUSSION

A. Layer morphology and photoluminescence as a function of the III/V ratio

The morphology and quality of the GaN layers grown by MBE on Si(111) depend strongly on the III/V ratio and the AlN buffer.² Figure 1 shows the GaN growth rate versus the Ga flux [beam equivalent pressure (BEP)] for growth temperatures between 660 and 770 °C and a fixed amount of active nitrogen (OED signal).^{3,4} For growth temperatures above 660 °C higher Ga fluxes are needed to reach the same growth rate, indicating a Ga desorption process from the layer surface.^{3,5–7} Due to this Ga desorption process the effective III/V ratio at the growth front will be equal to or smaller than the BEP ratio, depending on the growth temperature.

Below stoichiometry (roughly defined as the III/V ratio at which the growth rate saturates in Fig. 1) the epitaxial growth proceeds nominally under N-rich conditions, always leading to columnar morphologies. These columns are

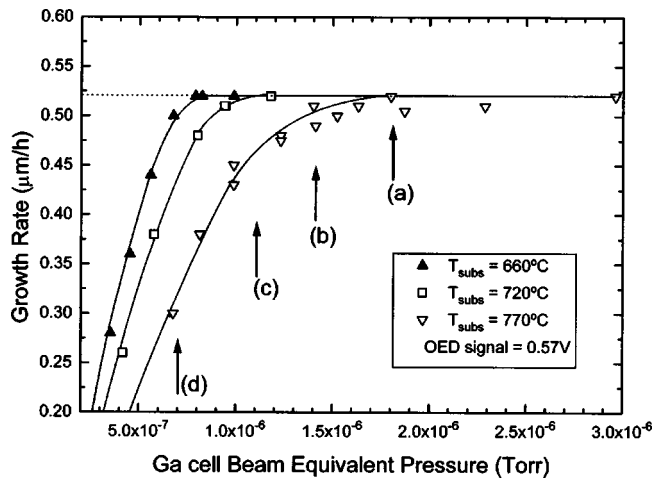


FIG. 1. GaN growth rate as a function of the Ga flux (beam equivalent pressure) for three different substrate temperatures and a given amount of active nitrogen. Solid lines are guides to the eye. Arrows show the III/V ratio for the growth conditions of the samples shown in Fig. 3.

aligned along the (0001) direction and have average diameters between 60 and 150 nm, either on Si(111) with or without AlN buffer, or on sapphire substrates⁸ (Fig. 2). Columnar morphologies were found to be typical of highly mismatched systems⁹ and, in the case of GaN, early reports on columnar structures were given by Gaskill, Bottka, and Lin¹⁰ in GaN grown by metal-organic vapor phase epitaxy (MOVPE) using hydrazine as a nitrogen source. More recently, Yoshizawa *et al.*¹¹ reported columnar GaN on sapphire grown by MBE assuming Ga-rich conditions, given the growth rate increase with the nitrogen flux. However, the Ga desorption rate at 800 °C is so high that the observed growth rate increase¹¹ with the nitrogen flux can be understood as the probability enhancement for Ga adatoms to encounter N adatoms for a successful incorporation to the crystal before being desorbed.⁵ For this reason, III/V ratios derived from BEP measurements may have no real meaning when there is a high Ga desorption rate. As a consequence, N-rich conditions at the surface may be reached either by decreasing the III/V BEP ratio, or by increasing the Ga desorption at high growth temperatures.

At stoichiometry, or under Ga-rich conditions, the GaN layer becomes compact [Fig. 3(a)]. Changes in morphology as a function of the III/V ratio are quite reproducible, and *mixed* GaN layers, first compact and then columnar, are grown starting at stoichiometry and following with a steplike reduction of the Ga flux. Columns also appear when increasing the growth temperature due to a Ga-desorption rate enhancement,^{5,12} although both methods may not be equivalent in terms of column density and size because the later method may increase the Ga adatoms surface diffusion. The density and diameter of the columns depend on how far the growth conditions lie below stoichiometry [Figs. 3(b)–3(d)], whereas the column height depends mainly on the growth time/rate. The arrows in Fig. 1 show the nominal, relatively N-rich growth conditions at 770 °C for different columnar morphologies: from high density-small diameter [highly N rich, Fig. 3(d)] to small density-large diameter [slightly N rich, Fig. 3(b)]. Our results agree with those by Yoshizawa

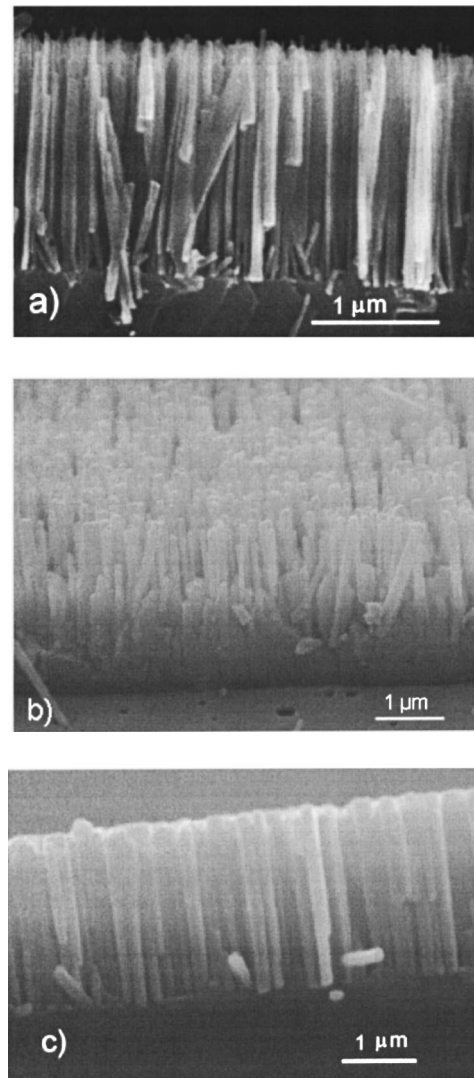


FIG. 2. SEM micrographs of GaN nanocolumns grown by MBE: (a) directly on Si(111); (b) on AlN-buffered Si(111), and (c) on GaN-buffered Al₂O₃.

*et al.*¹¹ and Yu *et al.*⁷ that show a column density reduction, together with a diameter increase, when going from N rich towards stoichiometry in GaN layers grown by MBE on Al₂O₃. This behavior may be understood as due to changes of the barrier that the N adatoms represent to the surface diffusion of the Ga adatoms.¹³

Figure 4 shows PL spectra of GaN samples with different columnar structures [Figs. 3(b)–3(d)]. Samples with a *high density of very thin* (<600 Å) columns [Fig. 3(d)] show PL spectra dominated by strong and narrow excitonic emissions at 3.472–3.478 eV [Fig. 4(a)]. The PL evolution with temperature shows the free-excitonic emissions A, B, and C and two excitonic emissions bound to neutral residual donors.¹⁴ These excitonic emissions fit with those found in relaxed, thick GaN layers.¹⁵ In addition, PL spectrum in Fig. 4(a) shows a partially resolved doublet at 3.450–3.456 eV and a broad emission at 3.41 eV.

In GaN samples with *lower density-higher diameter* columns [Fig. 3(c)], grown closer to stoichiometry either on Si(111) or sapphire, the doublet peaks slightly blueshift to 3.452–3.458 eV having a much higher relative intensity

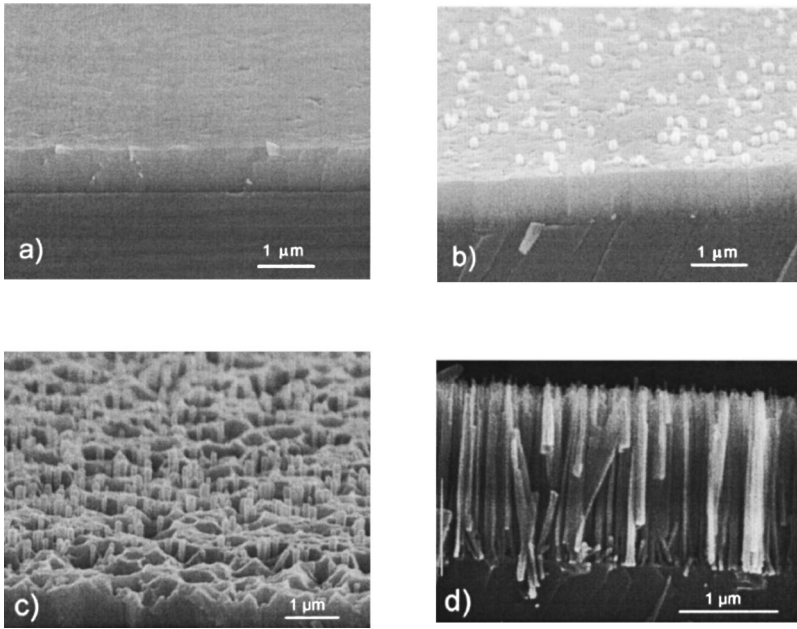


FIG. 3. SEM micrographs of GaN layer morphology as a function of the III/V ratio: (a) under slightly Ga-rich conditions or at stoichiometry; (b) slightly under stoichiometry towards N rich; (c) farther from stoichiometry towards N rich; and (d) far apart from stoichiometry towards N rich. These conditions are indicated in Fig. 1 as (a), (b), (c), and (d).

[Figs. 4(b) and 4(c)]. In those samples, the broad peak at 3.41 eV is still present with similar intensities as before.

Growth just below stoichiometry leads to the *lowest density-highest diameter* columns, with PL spectra similar to that in Fig. 4(b). However, when the *column's height is quite small* [small growth time, Fig. 3(b)] the excitonic emissions become weaker (small scattering volume) rendering the peak at 3.41 eV dominant [Fig. 4(d)]. This emission shows a

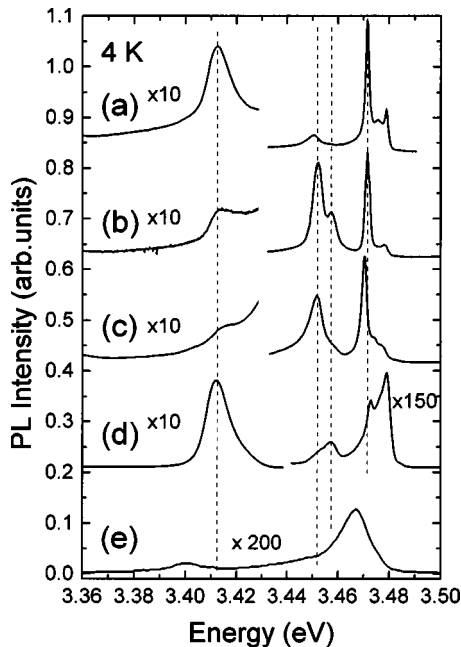


FIG. 4. Low-temperature PL spectra of GaN layers having different morphologies: (a) Very thin-very high density columns on Si(111). Strong N-rich conditions [Fig. 3(d)] (b) Wider-high density columns on Si(111). Less N-rich conditions [Fig. 3(c)]. (c) Same as (b) but grown on sapphire [in Fig. 2(c)]. Notice that the doublet is not resolved at 4 K, but it is resolved at 40 K with the same energy separation between peaks. (d) Wider-low density, *short* columns on Si(111). Slightly N-rich conditions [Fig. 3(b)]. (e) Compact GaN layer on Si(111). At stoichiometry or slightly Ga rich [Fig. 3(a)].

sample-dependent energy dispersion from 3.40 to 3.42 eV, and it also appears in compact GaN layers [Fig. 4(e)] where the biaxial tensile strain redshifts the PL spectrum.^{4,8} The following analysis will show that the emission at 3.41 eV originates at the disordered GaN column/substrate interface.

Time-resolved PL tuned at 3.472 and 3.455 eV yield similar exponential decays and lifetimes typical of an excitonic character (Fig. 5). However, the decay of the line at 3.416 eV is nonexponential with a longer lifetime, typical of a multi-component emission and/or a nonexcitonic character. In the following sections the doublet at 3.450–3.456 eV (or 3.452–3.458 eV) and the broad peak emerging at around 3.41 eV will be analyzed in detail.

B. Photoluminescence doublet at 3.452 and 3.458 eV

The PL emission doublet at 3.450–3.456 eV observed in GaN samples with *very-thin-very-high density* columns as a small contribution [Fig. 4(a)], becomes stronger and slightly blueshifted to 3.452–3.458 eV [Fig. 4(b)] in samples grown closer to stoichiometry where the columns have a *lower density higher diameter*. The energy difference between the doublet components is always the same and the doublet energy position is very reproducible with the growth conditions and morphology, whatever the substrate used [Figs. 4(b) and 4(c)]. This is clear evidence that the GaN columns are relaxed, since thin GaN layers grown on Si(111) or on sapphire are under biaxial tensile or compressive strain, respectively, leading to opposite energy shifts.^{15,16} RS data show unambiguously that the GaN nanocolumns, grown either on Si(111) or sapphire substrates, are fully relaxed (E_2 phonon at 568.0 cm^{-1}).

The excitonic emissions intensity (band edge and doublet) scale the density of columns (Fig. 6), providing clear evidence that they originate at the columns. In addition, CL signals tuned at 3.473 and 3.454 eV show up as bright spots that coincide with *the same column sites* observed by SEM [Figs. 7(a) and 7(b)]. CL data vs the electron beam energy (excitation depth) show a rather constant intensity along the columns for the excitonic emissions (Fig. 8), whereas the

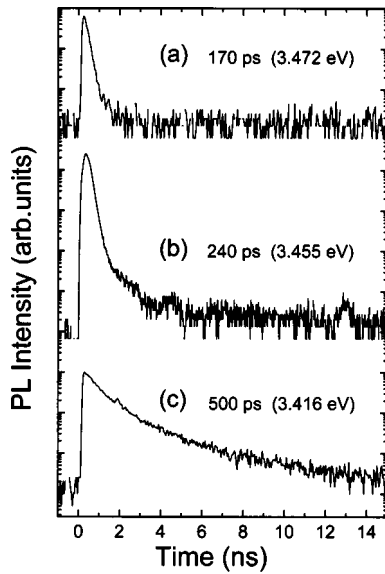


FIG. 5. Time dependence of PL peaks at 3.472, 3.455, and 3.410 eV.

signal at 3.41 eV keeps on increasing with the electron beam energy, becoming dominant at 15 KeV. At this energy the electrons are mostly sensing the columns bottom interface (Fig. 8 insert) and beyond this value all CL signals start to fade out. These results prove that the emissions at 3.473 and 3.454 eV originate at the column's volume, so that, they cannot be considered the same emission process, under different residual strain, coming from the columns and the compact regions in between. The same conclusion is reached from PL spectra in Figs. 4(b) and 4(c) corresponding to GaN columns grown on Si(111) and sapphire.

PL temperature and excitation power dependencies in Figs. 9(a) and 9(b) reveal that (i) the doublet peak energies do not shift with power and they follow the temperature band

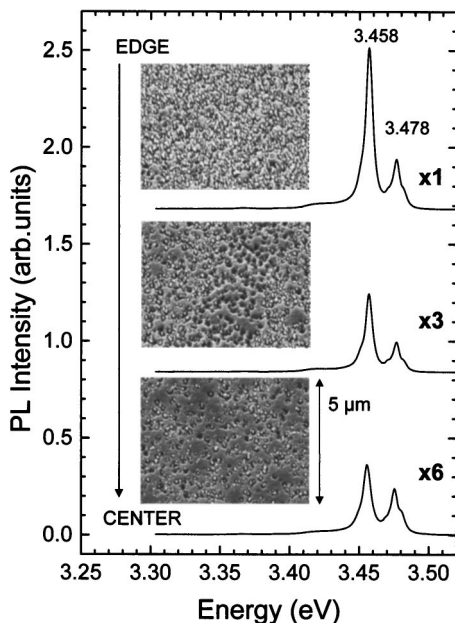


FIG. 6. Low- T (4 K) PL spectra intensity from a sample similar to that in Fig. 4(b) as a function of the column density measured by SEM.

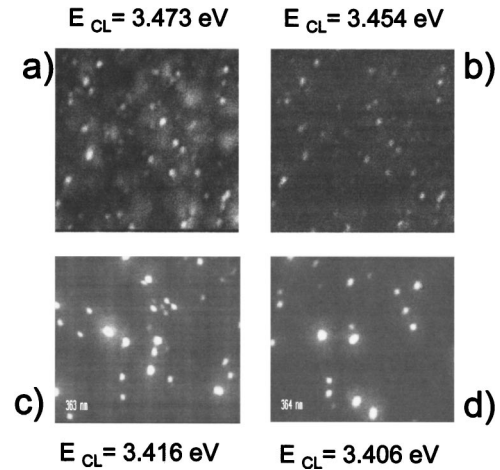


FIG. 7. 10 K CL images of nanocolumns taken at: (a) 3.473 eV; (b) 3.454 eV; (c) 3.416 eV; and (d) 3.406 eV.

gap dependence; (ii) the energy difference between the doublet peaks (6 meV) keeps constant with temperature and excitation; (iii) the intensity of the doublet high-energy component increases (relative to the low-energy component) with temperature/excitation power, as does the free exciton B with respect to the free exciton A ; and (iv) the doublet intensity drops at about the same temperature at which the donor-bound exciton D^0X_2 does. These features together with time-resolved PL data (Fig. 5), suggest an excitonic nature of the doublet bound to a donor (acceptor) and involving the A and B valence bands. Moreover, the similarity of the binding energies (E_A, E_B) derived from the thermal quenching of the doublet intensities [inset in Fig. 9(a)] points to a common impurity/defect. The doublet high relative intensity [Figs. 4(b) and 4(c)] rules out a two-electron replica of the free and donor-bound excitons at 3.472–3.478 eV.¹⁴

Considered as a *donor-bound exciton* the doublet position gives a donor optical depth of 130 meV (Hayne's rule¹⁷). *Experimental* data on impurities or point defects generating donors at 100 meV from the CB are scarce and not conclusive,^{18,19} and the most common *donor* species in GaN (O and Si) behave as shallow donors.^{20–23} Besides, O is not a usual contaminant in MBE-grown GaN, and Si contamination, plausible when using a Si(111) substrate, can be disregarded when growing on sapphire [Fig. 4(c)]. Similar PL doublets were found in thick (63 μm) relaxed GaN layers grown by HVPE (Ref. 24) and on thin GaN layers grown by MOVPE,²⁵ both on sapphire.

As an *acceptor-bound exciton* the doublet localization energy yields an acceptor optical depth of 260–270 meV (Hayne's rule¹⁷). Carbon is a common contaminant in MOVPE and MBE techniques, but *carbon-doped*⁸ GaN layers grown by MBE show an acceptor optical depth of 230 meV, in agreement with previous data,^{26,27} but significantly lower than the above values. Given the high purity of the solid sources, carbon (or other acceptors) *contamination* cannot be sustained in Figs. 4(b) and 4(c) where the doublet intensity equals that of the band edge emissions.

A careful analysis of the PL spectrum from a columnar GaN/Si(111) sample [Fig. 10(a)] shows (i) a first and second order LO-phonon replica of the doublet at 3.452–3.458 eV located at 3.368 and 3.276 eV, respectively; (ii) a first and

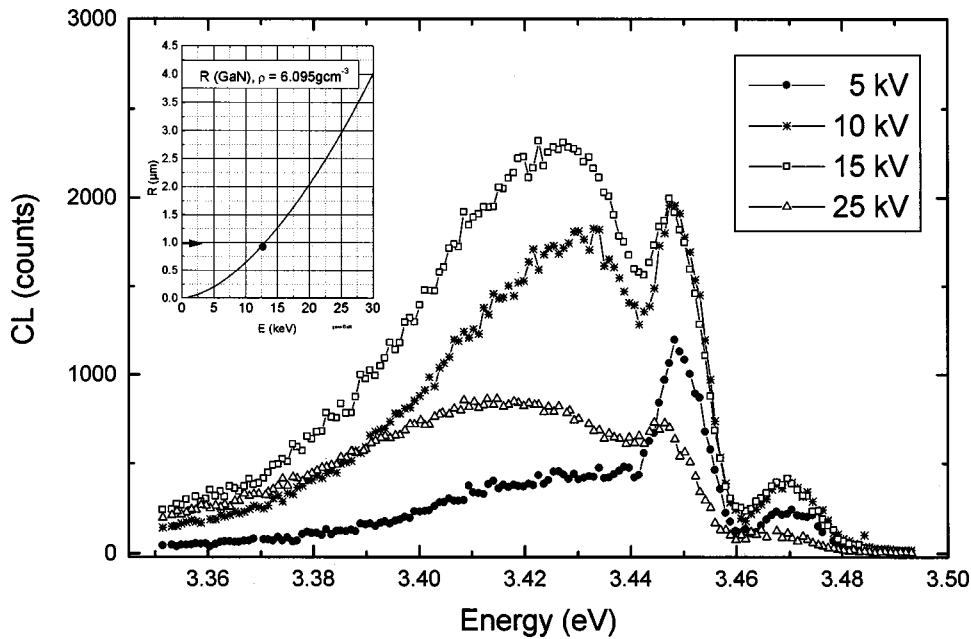


FIG. 8. 10 K CL spectra as a function of the electron beam energy in a columnar GaN sample (PL in Fig. 4(b)). The inset shows the electron penetration depth vs electron energy.

second order LO-phonon replica of the emission at 3.415 eV located at 3.324 and 3.234 eV, respectively; (iii) a second order LO-phonon replica of the FXA (or FXB) located at 3.298 eV (the first order one may be the shoulder at 3.388 eV); and (iv) a weak emission at 3.214 eV with a LO-phonon replica at 3.125 eV. The PL spectrum in Fig. 10(b) from a columnar GaN/Al₂O₃ sample shows essentially the same features. We conclude that these samples do not have significant traces of carbon or other acceptor impurities.

Theory predicts that point defects like V_N and Ga_I generate effective-masslike shallow donors.^{28–32} The energy position of the V_N donor state, generally taken as 29–35 meV,³³ is still uncertain, and there is even less evidence of the Ga_I related donor state position. However, neither V_N nor Ga_I defects may likely form in GaN layers grown under *real* N-rich conditions due to their high formation energies, but instead, N_{Ga} , N_I , or V_{Ga} . Although there is less agreement in the literature about the electronic structure and energy levels of the later defects, all predictions point to rather deep states.^{28,29,31}

Taking a closer look at the column growth process and its dependence with growth conditions, it seems quite plausible that the column growth starts from liquid Ga clusters at the substrate surface, produced by the Ga surface diffusion restriction imposed by the N excess.¹³ Indeed, this is the case shown by Guha *et al.*³⁴ when growing GaN columns selectively on Si/SiO₂ from liquid Ga clusters (Ga balling). This mechanism will grow the columns actually under *Ga-rich conditions* and this explains why a reduced N flux promotes the growth of wider columns due to the diffusion enhancement of the Ga adatoms (wider Ga clusters). Considering what kind of point defect this growth process would lead to, it is also sensible to think that the column surface would be defect free because of the lack of dislocations and the availability of N atoms close to the Ga-ball surface. On the other hand, N may not go easily through the Ga ball, so that, the column volume (inner part) may have Ga_I defects. In that case, the PL signals corresponding to the band edge excitonic emission (3.472–3.478 eV) would come mostly from

the column's surface, whereas the lower energy doublet may come from the inner part of the columns. CL spectra do not differentiate between column surface and volume. The surface-to-volume ratio of the columns follows the reciprocal of the column radius and the PL intensity ratio between the band edge emission and the doublet (3.452–3.458 eV) follows this trend quite accurately. This does not mean that the density of Ga_I defects increases when growing closer to “stoichiometry,” but just a geometrical effect that ponders more the column volume versus its surface. It is worthwhile to mention that quite different crystal qualities have been observed in GaN small pyramids, depending on the location sampled.³⁵ Considering the Ga-balling growth mode for the columns, it seems reasonable to think of Ga_I as the point defects responsible for the PL doublet at 3.452–3.458 eV, even though the measured III/V flux ratio (BEP) gives nominally N-rich conditions.

C. Photoluminescence peak at 3.41 eV

Figure 4 shows a PL emission peak at 3.41 eV, typically found in compact or columnar GaN grown on Si(111) or sapphire. This emission becomes dominant in columnar GaN with very short columns [Figs. 3(b) and 4(d)] because of a strong reduction of the band edge emissions by a reduced scattering volume (see the intensities of the 3.41-eV peak in Fig. 4). The intensity of the 3.41-eV emission scales the density of columns (Fig. 11) and CL signals tuned at energies close to 3.41 eV reveal bright spots corresponding to the column sites (Fig. 7). In addition, the CL intensity of this emission increases significantly as the electron beam senses the column in depth (Fig. 8). These facts point to the columns as the origin of this emission, more precisely, from the column bottom interface. This location explains why the intensity of the emission at 3.41 eV is barely affected by the column height reduction.

From the dependence of the 3.41-eV PL emission on temperature and excitation power in columnar GaN, Calle *et al.*¹⁴ suggested a DAP character leading to an acceptor

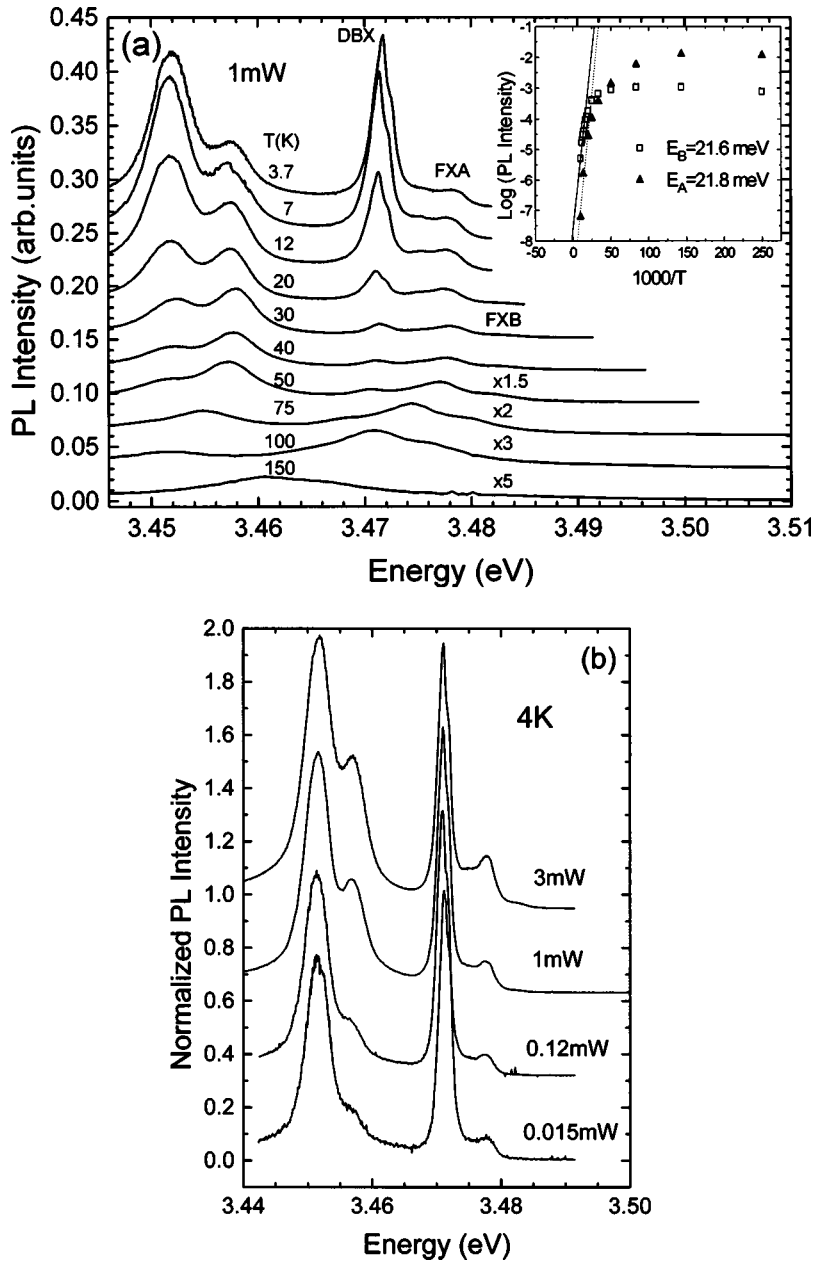


FIG. 9. (a) Temperature and (b) excitation power dependence of the band edge (3.472–3.478 eV) and doublet (3.452–3.458 eV) PL intensities from a columnar GaN layer [Fig. 4(b)]. The inset shows the thermal quenching of the doublet peaks.

optical depth of 70 meV, in agreement with previous reports.³⁶ Time-resolved PL data in Fig. 5 give rather long (500 ns) nonexponential decays, while the peak redshifts by 4 meV after 8 ns from the laser pulse. Similar redshifts are shown by Smith *et al.*³⁷ for PL emissions between 3.414 and 3.420 eV in GaN/Al₂O₃, and Godlewski *et al.*³⁸ attributed an emission at 3.414 eV to a “shallow” DAP or a free-to-bound recombination.

PL emissions at 3.41–3.42 eV were reported on GaN/Al₂O₃ grown by MBE with a partially resolved fine structure in some cases.^{37,39–41} A previous assignment of this emission to oxygen⁴² can be ruled out by the work of Niebuhr *et al.*⁴³ in O-doped GaN/Al₂O₃. Moreover, the work by Fisher *et al.*⁴⁴ analyzes a “family” of four PL peaks around 3.41 eV in GaN grown on sapphire and SiC, concluding that these features have no relation with oxygen, but rather to *structural defects*, since they show up in GaN samples after Ar⁺ implantation. They report nonexponential PL decays quite similar to those in Fig. 5, and a strong PL signal enhancement when the layers were excited from the back side

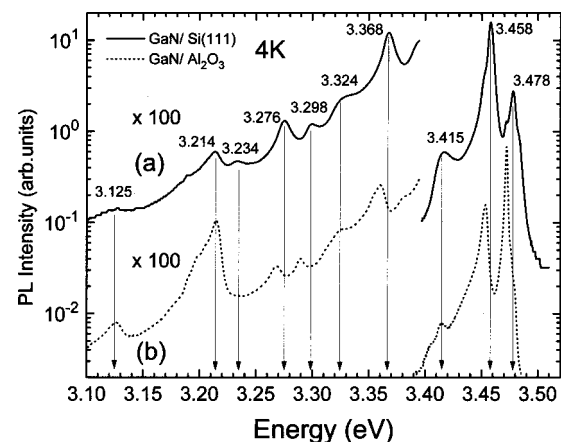


FIG. 10. Detailed low-temperature (4 K) PL spectra of GaN nanocolumns grown on (a) Si(111) and (b) sapphire substrates.

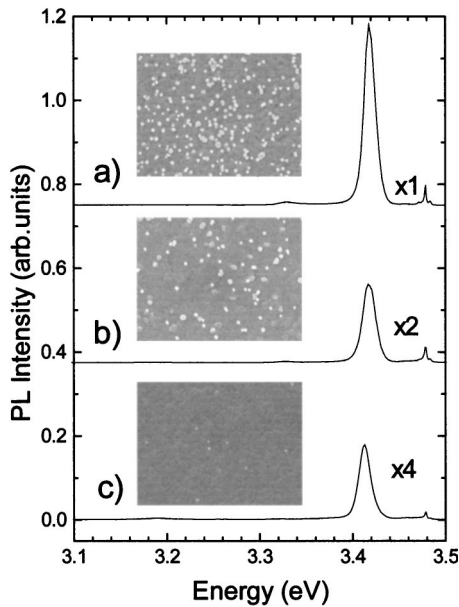


FIG. 11. Correlation between the low- T (4 K) PL intensity of the emission at 3.41 eV and the density of columns (plan view SEM).

(sapphire), in good agreement with our CL data as a function of the electron beam energy (Fig. 8).

A spectral energy dispersion has been often reported for this emission line (3.407–3.424 eV) as a function of the

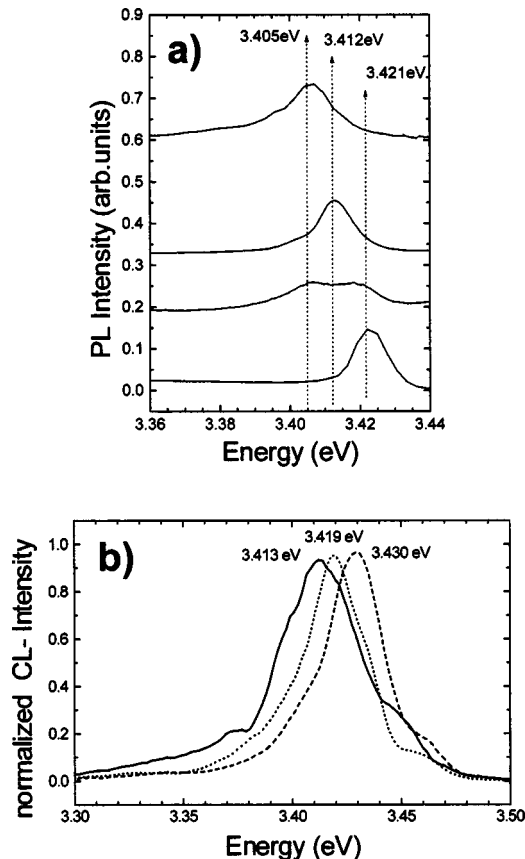


FIG. 12. Spectral energy dispersion of the emission at 3.41 eV measured by (a) PL from sample to sample, and (b) by CL as a function of the electron beam spot location.

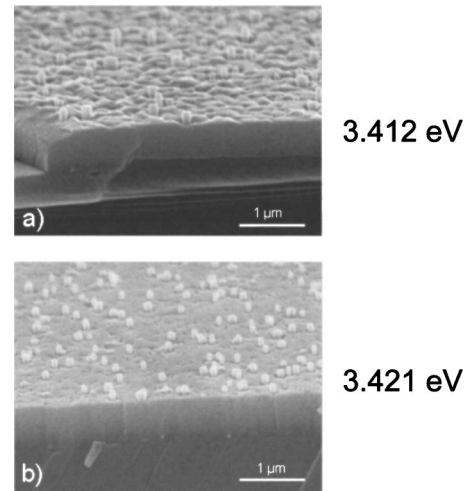


FIG. 13. SEM micrographs of GaN nanocolumns lying on (a) a rough surface (craters) and (b) a flat surface.

excitation, as well as from sample to sample.^{37,39,41,42,44} Fisher *et al.*⁴⁴ observed a partially resolved structure on the 3.42-eV PL peak suggesting the participation of the nondegenerate valence bands. We have observed this spectral energy dispersion from sample to sample without an apparent correlation with the growth conditions. Figure 12(a) shows PL spectra from various samples where the dominant peaks lie at different (but close) energies, from 3.405 to 3.421 eV. Similarly, CL spectra taken on different columns on the same sample shift from 3.413 to 3.430 eV [Fig. 12(b)]. Figures 7(c) and 7(d) show that the bright spots from CL, tuned at 3.416 and 3.406 eV, do not correspond to the same columns. Since all columns are relaxed and the defects giving rise to these emissions are located at the column bottom interface, we attribute the observed spectral energy dispersion to interactions of these defects with local strain fields and/or electric fields associated with close dislocations present at the column's bottom interface.⁴⁵ A recent work by Cheng *et al.*⁴⁶ evidences the dependence of this spectral energy dispersion on the substrate employed, namely sapphire, SiC, and GaN/SiC, that may well be related to different strain fields neighboring the structural defects. We have determined, as a general trend, that columns lying on very rough compact material (i.e., columns inside craters) show preferentially the emission line around 3.410 eV [Fig. 13(a)], whereas columns lying on flatter surfaces exhibit the emission line at 3.420 eV [Fig. 13(b)]. We cannot further elaborate on the origin and type of these defects from the available experimental data.

In summary, a reproducible method to grow GaN nanocolumns by MBE is presented, with control on the column density and diameter. The luminescence doublet at 3.452–3.458 eV, typically observed in columnar structures, has an excitonic character and involves the A and B valence bands. Considering the Ga-balling model for the column's growth, Ga-interstitials seem to be the most probable point defects related to these emissions. The broad emission at 3.41 eV arises from structural defects at the column/substrate interface. The interaction of these point defects with strain and/or electric fields associated with dislocations seems to be a plausible explanation for the observed sample-dependent energy dispersion. A clear relation between the specific emission energy and the layer morphology underneath the columns is found.

ACKNOWLEDGMENTS

The authors wish to acknowledge the Raman characterization by J. Sánchez and J. M. Calleja, and the time-

resolved PL measurements by C. H. Molloy and D. J. Sommerford. Financial support was provided by CICYT Projects Nos. TIC95-0770, MAT98-0823-C03-01, MAT98-0823-C03-02, and EU ESPRIT LTR Project 20968 (Laquani).

- ¹S. Nakamura, M. Senoh, S. I. Nagahama, N. Iwasa, T. Yamada, T. Matsushita, H. Kiyoku, Y. Sugimoto, T. Kozaki, H. Umemoto, M. Sano, and K. Chocho, *Appl. Phys. Lett.* **72**, 2014 (1998).
- ²E. Calleja, M. A. Sánchez-García, E. Monroy, F. J. Sánchez, E. Muñoz, A. Sáenz-Hervás, C. Villar, and M. Aguilar, *J. Appl. Phys.* **82**, 4681 (1997).
- ³M. A. Sánchez-García, E. Calleja, E. Monroy, F. J. Sánchez, F. Calle, E. Muñoz, and R. Beresford, *J. Cryst. Growth* **183**, 23 (1998).
- ⁴E. Calleja, M. A. Sánchez-García, D. Basak, F. J. Sánchez, F. Calle, P. Youinou, E. Muñoz, J. J. Serrano, J. M. Blanco, C. Villar, T. Laine, J. Oila, K. Saarinen, P. Hautajarvi, C. H. Molloy, D. J. Sommerford, and I. Harrison, *Phys. Rev. B* **58**, 1550 (1998).
- ⁵S. Guha, N. A. Bojarczuk, and D. W. Kisker, *Appl. Phys. Lett.* **69**, 2879 (1996).
- ⁶R. C. Powell, N. E. Lee, Y. W. Kim, and J. E. Greene, *J. Appl. Phys.* **73**, 189 (1993).
- ⁷Z. Yu, S. L. Buczkowski, N. C. Giles, T. H. Myers, and M. R. Richards-Babb, *Appl. Phys. Lett.* **69**, 2731 (1996).
- ⁸E. Calleja, M. A. Sánchez-García, F. J. Sánchez, F. Calle, F. B. Naranjo, E. Muñoz, S. I. Molina, A. M. Sánchez, F. J. Pacheco, and R. García, *J. Cryst. Growth* **201/202**, 296 (1999).
- ⁹I. Akasaki, H. Amano, H. Murakami, M. Sassa, H. Kato, and K. Manabe, *J. Cryst. Growth* **128**, 379 (1993).
- ¹⁰D. K. Gaskill, N. Bottka, and M. C. Lin, *Appl. Phys. Lett.* **48**, 1449 (1986).
- ¹¹M. Yoshizawa, A. Kikuchi, M. Mori, N. Fujita, and K. Kishino, *Jpn. J. Appl. Phys., Part 2* **36**, L459 (1997).
- ¹²R. Birkhahn and A. J. Steckl, *Appl. Phys. Lett.* **73**, 2143 (1998).
- ¹³T. Zywietz, J. Neugebauer, and M. Scheffler, *Appl. Phys. Lett.* **73**, 487 (1998).
- ¹⁴F. Calle, F. J. Sánchez, J. M. Tijero, M. A. Sánchez-García, E. Calleja, and R. Beresford, *Semicond. Sci. Technol.* **12**, 1396 (1997).
- ¹⁵D. Volm, K. Oettinger, T. Streibl, D. Kovalev, M. Ben-Chorin, J. Diener, B. K. Meyer, J. Majewski, L. Eckey, A. Hoffmann, H. Amano, I. Akasaki, K. Hiramatsu, and D. T. Detchprohm, *Phys. Rev. B* **53**, 16 543 (1996).
- ¹⁶W. Shan, R. J. Hauenstein, A. J. Fischer, J. J. Song, W. G. Perry, M. D. Bremser, R. F. Davis, and B. Goldenberg, *Phys. Rev. B* **54**, 13 460 (1996); A. Shikanai, T. Azuhata, T. Sota, S. Chichibu, A. Kuramata, K. Horino, and S. Nakamura, *J. Appl. Phys.* **81**, 417 (1997).
- ¹⁷J. R. Haynes, *Phys. Rev. Lett.* **4**, 361 (1960).
- ¹⁸V. S. Vavilov, S. I. Makarov, M. V. Chukichev, and I. F. Chetverikova, *Fiz. Tekh. Poluprovodn.* **13**, 2153 (1979) [*Sov. Phys. Semicond.* **13**, 1259 (1979)].
- ¹⁹T. L. Tansley and R. J. Egan, *Phys. Rev. B* **45**, 10 942 (1992).
- ²⁰T. Mattila and R. M. Nieminen, *Phys. Rev. B* **54**, 16 676 (1996).
- ²¹C. Wetzel, T. Suski, J. W. Ager, E. R. Weber, E. E. Haller, S. Fischer, B. K. Meyer, R. J. Molnar, and P. Perlin, *Phys. Rev. Lett.* **78**, 3923 (1997).
- ²²M. Ramsteiner, J. Menniger, O. Brandt, H. Yang, and K. H. Ploog, *Appl. Phys. Lett.* **69**, 1276 (1996).
- ²³J. C. Zolper, R. G. Wilson, S. J. Pearson, and R. A. Stall, *Appl. Phys. Lett.* **68**, 1945 (1996).
- ²⁴G. E. Bunea, W. D. Herzog, M. S. Ünlü, B. B. Goldberg, and R. J. Molnar, *Appl. Phys. Lett.* **75**, 838 (1999).
- ²⁵B. Beaumont (private communication).
- ²⁶S. Fischer, C. Wetzel, E. E. Haller, and B. K. Meyer, *Appl. Phys. Lett.* **67**, 1298 (1995).
- ²⁷M. Leroux, B. Beaumont, N. Grandjean, C. Golivet, P. Gibart, J. Massies, J. Leymarie, A. Vasson, and A. M. Vasson, *Mater. Sci. Eng., B* **50**, 97 (1997).
- ²⁸P. Boguslawski, E. L. Briggs, and J. Bernholc, *Phys. Rev. B* **51**, 17 255 (1995).
- ²⁹D. W. Jenkins and J. D. Dow, *Phys. Rev. B* **39**, 3317 (1989); See also D. W. Jenkins, J. D. Dow, and M. H. Tsai, *J. Appl. Phys.* **72**, 4130 (1992).
- ³⁰T. Mattila and R. M. Nieminen, *Phys. Rev. B* **55**, 9571 (1997).
- ³¹J. Neugebauer and C. G. Van de Walle, *Phys. Rev. B* **50**, 8067 (1994).
- ³²P. Perlin, T. Suski, M. Leszczynski, I. Grzegory, J. Jun, S. Porowski, P. Boguslawski, J. Bernholc, J. C. Chervin, A. Polian, and D. Moustakas, *Phys. Rev. Lett.* **75**, 296 (1995).
- ³³M. Ilegems and H. C. Montgomery, *J. Phys. Chem. Solids* **34**, 885 (1973).
- ³⁴S. Guha, N. A. Bojarczuk, M. A. L. Johnson, and J. F. Schetzina, *Appl. Phys. Lett.* **75**, 463 (1999).
- ³⁵K. C. Zeng, J. Y. Lin, H. X. Jiang, and W. Yang, *Appl. Phys. Lett.* **74**, 1227 (1999).
- ³⁶B. G. Ren, J. W. Orton, T. S. Cheng, D. J. Dewsnip, D. E. Lacklison, C. T. Foxon, C. H. Malloy, and X. Chen, *MRS Internet J. Nitride Semicond. Res.* **1**, 22 (1996).
- ³⁷M. Smith, G. D. Chen, J. Y. Lin, H. X. Jiang, A. Salvador, B. N. Sverdlov, A. Botchkarev, and H. Morkoç, *Appl. Phys. Lett.* **66**, 3474 (1995).
- ³⁸M. Godlewski, J. P. Bergman, B. Monemar, U. Rossner, and A. Barski, *Appl. Phys. Lett.* **69**, 2089 (1996).
- ³⁹A. V. Andrianov, D. E. Lacklison, J. W. Orton, D. J. Dewsnip, S. E. Hooper, and C. T. Foxon, *Semicond. Sci. Technol.* **11**, 366 (1996).
- ⁴⁰S. Fischer, C. Wetzel, W. L. Hansen, E. D. Bourret-Courchesne, B. K. Meyer, and E. E. Haller, *Appl. Phys. Lett.* **69**, 2716 (1996).
- ⁴¹G. D. Chen, M. Smith, J. Y. Lin, H. X. Jiang, A. Salvador, B. N. Sverdlov, A. Botchkarev, and H. Morkoç, *J. Appl. Phys.* **79**, 2675 (1996).
- ⁴²B. C. Chung and M. Gershenson, *J. Appl. Phys.* **72**, 651 (1992).
- ⁴³R. Niebuhr, K. H. Bachem, U. Kaufmann, M. Maier, C. Merz, B. Santic, P. Schlotter, and H. Jürgensen, *J. Electron. Mater.* **26**, 1127 (1997).
- ⁴⁴S. Fischer, G. Steude, D. M. Hofmann, F. Kurth, F. Anders, M.

- Topf, B. K. Meyer, F. Bertram, M. Schmidt, J. Christen, L. Eckey, J. Holst, A. Hoffmann, B. Mensching, and B. Rauchenbach, *J. Cryst. Growth* **189/190**, 556 (1998).
- ⁴⁵J. Neugebauer and C. G. Van de Walle, *Appl. Phys. Lett.* **69**, 503 (1996).
- ⁴⁶T. S. Cheng, C. T. Foxon, G. B. Ren, J. W. Orton, Yu V. Melnik, I. P. Nikitina, A. E. Nikolaev, S. V. Novikov, and V. D. Dimitriev, *Semicond. Sci. Technol.* **12**, 917 (1997).